TECHNICAL MEMORANDUM

301

Development of linearized radiation and cloud schemes for the assimilation of cloud properties

M. Janisková, J-F. Mahfouf,
J-J. Morcrette and F. Chevallier

Research Department

March 2000

European Centre for Medium-Range Weather Forecasts
Europäisches Zentrum für mittelfristige Wettervorhersage
Centre européen pour les prévisions météorologiques à moyen

Abstract

A proper consideration of cloud-radiation interactions in the linearized model is required for preparing the assimilation of cloud properties in the framework of the 4D-Var system. The development of a linearized cloud scheme and a radiation scheme taking into account cloudiness has been done.

The tangent-linear and adjoint versions of the ECMWF shortwave radiation scheme have been developed without a priori modifications. A combination of artificial neural networks and Jacobian matrices has been defined for the linearized longwave radiation scheme. For the time being, a diagnostic cloud scheme has been linearized to be used with radiation.

The accuracy of the linearization of both radiation and diagnostic cloud schemes has been examined. The inclusion of more sophisticated radiation to existing linearized parametrizations improves the fit to the nonlinear model. However, impact of the linearized diagnostic cloud scheme is small. Therefore the linearized model will require an improved cloud parametrization.

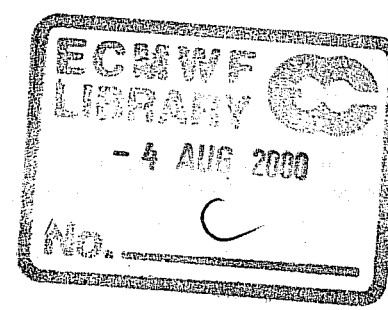

1 Introduction

Current operational data assimilation systems only account for conventional observations and clear-sky satellite radiances. They do not explicitly include any quantity related to the condensed phase of water as cloud water, cloud ice or rain. The inclusion of cloud observations in the ECMWF data assimilation would lead to an improved initial state of the prognostic variables which could in turn improve the quality of the forecasts (two-meter temperature, cloudiness, precipitation, ...). Data from future satellite missions (ERM [1], CLOUDSAT, PICASSO-CENA [2]) or field experiments (CLARE [3], ARM [4], LITE [5]) will be used to perform feasibility studies on the assimilation of cloud properties.

The 4D-Var assimilation system implemented in November 1997 (Rabier *et al.* 1999, Mahfouf and Rabier 1999) at ECMWF is flexible enough to allow for the assimilation of new types of observations. Some studies on assimilating rainfall data from the recently launched TRMM [6] satellite into the ECMWF analysis and forecasting system have been done by Marécal and Mahfouf (1999). A similar approach might be taken for the assimilation of cloud data from current and future satellite missions. However, this requires the definition of an observation operator that provides the model counterpart of the cloud observations. The observation operators for the assimilation of cloud properties and top of atmosphere fluxes are the linearized versions of both a radiative transfer model and a cloud scheme. Their linearized versions need to be developed for use in variational data assimilation.

Radiative transfer models in clear sky do not describe strong non-linear processes (even though some saturation effects can take place in water vapour absorption bands). Thus linearized radiation codes have been used successfully for a variational assimilation of clear-sky radiances in NWP models (for example Eyre, 1995).

The linearization of physical parametrization schemes describing cloud processes and cloud-radiation interactions is not straightforward since the on/off nature of clouds can make the tangent-linear approximation questionable. Janisková *et al.* (1999) reported results on the linearization of a simple diagnostic cloud scheme for use in a global atmospheric model. Due to the presence of thresholds in the cloud scheme, considerable noise in the solution was observed. Therefore the perturbations in cloud cover were neglected in that study. More encouraging results were obtained at smaller scale (Verlinde and Cotton, 1993; Park and Droegemeier, 1997) where linearized versions of cloud resolving models have been developed with some success for radar retrievals applications.

[1] Earth Radiation Mission

[2] Pathfinder Instruments for Cloud and Aerosol Spaceborne Observations - Climatologie Etendue des Nuages et des Aerosols

[3] Cloud Lidar and Radar Experiment

[4] Atmospheric Radiation Measurement

[5] Lidar In-space Technology Experiment

[6] Tropical Rainfall Measuring Mission

In this study, the development of comprehensive linearized radiation and cloud schemes is presented. In section 2, a brief description of shortwave and longwave radiation is done with emphasis on the incorporation of the effects of clouds on the radiation fluxes. The linearized diagnostic cloud scheme is also described there. The validation of the tangent linear model including cloud-radiation processes together with solving threshold problem in the cloud scheme is given in section 3. The study concludes with a brief summary of the results.

2 Development of the linearized radiation and cloud schemes

A very simplified linearized longwave radiation code is currently used in the ECMWF operational 4D-Var. Radiative transfer for the long-wave spectrum is modeled using a constant emissivity formulation where effective emissivity arrays are stored from the full non-linear radiation scheme (Mahfouf, 1999). The net longwave radiation at any level then strongly depends on the temperature on that level. In this approach, no dependency of radiation on cloudiness is taken into account. A proper consideration of cloud-radiation interactions requires the development of a linearized cloud scheme and a more sophisticated radiation scheme, which enables to take into account cloudiness.

2.1 The shortwave radiation scheme

The shortwave radiation scheme, originaly developed by Fouquart and Bonnel (1980) is used in the ECMWF physical parametrization (Morcrette, 1989 and 1991). It uses the photon-path-distribution method to separate the parametrization of the scattering processes from that of molecular absorption. Upward and downward fluxes are obtained from the reflectance and transmittances of the atmospheric layers. Solar radiation is absorbed by gases as water vapour, oxygen, carbon dioxide, methane, nitrous oxide and ozone, and scattered by molecules (Rayleigh scattering), aerosols and cloud particles. To perform the spectral integration, the solar spectral interval is discretized into subintervals in which the surface reflectance is considered as constant. Since the main cause of the important spectral variation of the surface albedo is the sharp increase in the reflectivity of the vegetation in the near infrared, and since water vapour does not absorb below 0.68 μm, the shortwave scheme considers two spectral intervals, one for the visible part (0.2 - 0.68 μm) and one for the near infrared (0.68 - 4.0 μm) part of the solar spectrum. This makes the scheme more computationally efficient since the interactions between gaseous absorption and scattering processes are accounted for only in the near-infrared interval.

Considering an atmosphere covered by clouds, the final fluxes are computed as a weighted average of the fluxes in the clear sky and in the cloudy fractions of the column (depending on cloud-overlap assumption). It is assumed that the atmosphere is divided into homogeneous

layers. The upward and downward fluxes at a given layer j are then given by

$$F^{\downarrow}_{sw}(j) = F_0 \prod_{k=j}^{N} \mathcal{T}_{bot}(k) \quad (1)$$

$$F^{\uparrow}_{sw}(j) = F^{\downarrow}_{sw}(j)\mathcal{R}_{top}(j-1) \quad (2)$$

where $\mathcal{R}_{top}(j)$ and $\mathcal{T}_{bot}(j)$ are the reflectance at the top and transmittance at the bottom of the jth layer. Computations of $\mathcal{T}_{bot}$ start at the top of the atmosphere and work downward. Those of $\mathcal{R}_{top}$ start at the surface and work upward. In the presence of cloud in the layer, $\mathcal{R}_{top}$ and $\mathcal{T}_{bot}$ are calculated as

$$\mathcal{R}_{top} = C_{cloud}\mathcal{R}_{cloud} + (1 - C_{cloud})\mathcal{R}_{clear} \quad (3)$$

$$\mathcal{T}_{bot} = C_{cloud}\mathcal{T}_{cloud} + (1 - C_{cloud})\mathcal{T}_{clear} \quad (4)$$

where C_{cloud} is the cloud fractional coverage of the layer within the cloudy fraction of the column.

In the cloudy fraction of the layer, the reflectance at the top and transmittance at the bottom of a cloudy layer are calculated with the Delta-Eddington approximation. These two quantities are calculated as functions of the total optical thickness δ (related to the cloud liquid/ice water amount), the single scattering albedo ω and the total assymetry factor g. These optical properties for clouds are derived from Fouquart (1987) and Ebert and Curry (1992).

The shortwave radiation scheme, briefly described above, is less expensive than ECMWF longwave radiation. This is why, this scheme was linearized without a priori modifications.

2.2 The longwave radiation scheme

The longwave radiation scheme, presently operational at ECMWF, is a band emissivity type scheme (Morcrette, 1990). The longwave spectrum from 0 to 2820 cm^{-1} is divided into six spectral regions. The transmission functions for water vapour and carbon dioxide over those spectral intervals are fitted using Padé approximations on narrow-band transmissions obtained with statistical band models (Morcrette *et al.*, 1986). Integration of the radiation transfer equation over wavenumber ν within the particular spectral regions gives the upward and downward fluxes.

The incorporation of the effects of clouds on the longwave fluxes follows the treatment discussed by Washington and Williamson (1997). The scheme calculates first upward and downward fluxes ($F^{\uparrow}_0(i)$ and $F^{\downarrow}_0(i)$) corresponding to a clear-sky atmosphere. In any cloudy layer, the scheme evaluates the fluxes assuming a unique overcast cloud of emissivity unity, i.e. $F^{\uparrow}_n(i)$ and $F^{\downarrow}_n(i)$ for a cloud present in the nth layer of the atmosphere. The fluxes for the actual atmosphere are derived from a linear combination of the fluxes calculated in the previous steps with some

cloud overlap assumption in the case of cloud present in several layers. Let N be the number of model layers starting from the top of atmosphere to the bottom (with levels counting from 0 to N in the same direction), C_i the fractional cloud cover in layer i, the cloudy upward $F_{lw}^{\uparrow}$ and downward $F_{lw}^{\downarrow}$ fluxes are expressed as:

$$F_{lw}^{\uparrow}(i) = (1 - CC_{N,i})F_0^{\uparrow}(i) + \sum_{k=i}^{N}(CC_{i,k+1} - CC_{i,k})F_k^{\uparrow}(i) \quad (5)$$

$$F_{lw}^{\downarrow}(i) = (1 - CC_{i-1,0})F_0^{\downarrow}(i) + \sum_{k=1}^{i-1}(CC_{i,k+1} - CC_{i,k})F_k^{\downarrow}(i) \quad (6)$$

where $CC_{i,j}$ is the cloudiness encountered between any two levels i and j in the atmosphere computed using a certain overlap assumption. The maximum-random overlap assumption is operationally used in the ECMWF model as follows

$$CC_{i,j} = 1 - \prod_{k=j+1}^{i}\left[\frac{1 - max(C_k, C_{k-1})}{1 - C_{k-1}}\right] \quad (7)$$

In the case of semi-transparent clouds, the fractional cloudiness entering the calculations is an effective cloud cover equal to the product of the emissivity due to condensed water and gases in the layer by the horizontal coverage of the cloud cover.

The complexity of the radiation scheme for the longwave part of the spectrum makes accurate computations expensive. To reduce its computational cost, simplifications are required in the assimilation framework. The longwave radiative fluxes depend upon temperature, water vapour, cloud cover and liquid and ice water contents. The design of the scheme allows to separate the contribution of temperature and water vapour from that of cloud parameters. Perturbations of radiative fluxes with respect to temperature and water vapour are obtained using pre-computed Jacobians averaged globally. Perturbations of radiative fluxes with respect to cloud parameters are computed using a tangent-linear scheme. The trajectory of radiative fluxes required in tangent-linear and adjoint computations are estimated efficiently from neural networks (Chevallier *et al.*, 1999).

More precisely, as described in the equations (5) and (6), the upward and downward longwave fluxes at height z_i can be expressed as:

$$F(z_i) = \sum_k a_k(z_i)F_k(z_i) \quad (8)$$

where the coefficients a_k are function of the cloudiness matrices $CC_{i,k}$. A differentiation of the above equation leads to:

$$dF(z_i) = \sum_k [a_k(z_i)dF_k(z_i) + F_k(z_i)da_k(z_i)] \quad (9)$$

Due to the weak non-linearities in the variations of the radiative fluxes F_k with respect to temperature and water vapour, the tangent-linear approximation can be used to compute ac-

curately finite-size perturbations ΔF_k from standard Jacobian matrices ($\partial F_k/\partial x$) as

$$\Delta F_k(z_i) \simeq \sum_x \sum_j \frac{\partial F_k(z_i)}{\partial x_j} \Delta x_j \tag{10}$$

where j represents the summation over the vertical layers and x are the atmospheric temperature and humidity profiles.

In the proposed approach, ΔF is approximated by:

$$\Delta F(z_i) \simeq \sum_k [a_k(z_i)\Delta F_k(z_i) + F_k(z_i)\Delta a_k(z_i)] \tag{11}$$

NL model — Jacobian matrices — NeuroFlux — TL model

Flux perturbations $\Delta F_k(z_i)$ are estimated using averaged Jacobian matrices (equation 10). Details on the averaging of this approximation can be found in Mahfouf *et al.* (1999). Δa_k is obtained by a linearization of those coefficients. In equation (11), fluxes from the basic state are also needed. In order to avoid significant extra memory storage or important recomputations, those fluxes are obtained using a neural network version (called NeuroFlux) of the ECMWF longwave radiative transfer model. The basic principles of this method can be found in Chéruy *et al.* (1996) and Chevallier *et al.* (1998).

2.3 The cloudiness parametrization scheme

For the time being, a diagnostic cloud scheme (Slingo, 1987) has been linearized to be used with linearized radiation.

The cloud scheme allows for four cloud types: convective cloud and three types of layer clouds (high, middle and low level). The convective cloud can fill any number of model layers and its depth is determined by the convection scheme. The computation is done using the scaled time-averaged precipitation rate ($\bar{P}$) from the model convection scheme.

The layered clouds can cover a number of model layers. In the case of high clouds, the scheme distinguishes between two types of cirrus, those associated with outflow from deep convection (parametrized from convective clouds) and those associated with frontal disturbance. Middle level clouds are generally characterized by moist air and large scale ascent. Low clouds are divided into those associated with extratropical fronts and tropical disturbances and those strongly linked to the boundary layer and invariably associated with low level inversions in temperature and humidity.

Extratropical and frontal cirrus as well as middle level clouds and low level clouds associated with extratropical fronts are determined from a function of the layer relative humidity (RH_e)

after following adjustment for the presence of convective clouds (C_{conv}) $RH_e = RH - C_{conv}$. Such modified relative humidity is then used as the basis for the decision of occurence of the layer clouds when the relative humidity reaches certain threshold value. The clouds are then parametrized using the function:

$$f(RH_e) = \left\{ max\left[\frac{RH_e - b}{1-b}, 0\right]\right\}^2 \tag{12}$$

where b is equal to 0.8 for high and middle level clouds and to 0.7 for low level cloud. In the case of middle level clouds and low level clouds associated with the extratropical fronts, the above function is modified by a linear transition up to weak ascent using vertical velocity. There are no such clouds in areas with subsidence.

Liquid water l_{lwc} and ice water l_{iwc} are proportional to specific humidity at saturation q_{sat}. They are defined as

$$l_{lwc} = \alpha l_{lc} \tag{13}$$
$$l_{iwc} = (1-\alpha) l_{lc} \tag{14}$$

where α is the fraction of condensate held as liquid water and $l_{lc} = f(C_i, q_{sat})$ with C_i being cloud cover of individual layer.

In the linearized version of the described diagnostic cloud scheme, there is some simplification coming from the fact that the current linearized convection scheme does not provide perturbations of precipitation. This leads to the zero perturbation of convective cloudiness. Some additional modification of the linearized cloud scheme had to be done (described later) in order to avoid the threshold problem in the parametrization of the layer clouds using the relative humidity dependency (see equation 12).

In the future, the aim is to use the adjoint of the prognostic cloud scheme (Tiedtke, 1993), in which the time evolution of cloud variables (cloud water content, cloud area) is directly linked to the various physical processes. Such developments are necessary not only to account for cloud-radiation interactions, but also to improve the coupling with the convection scheme for the assimilation of precipitation. However, the linearization of cloud schemes is not straightforward because of the on/off nature of the clouds.

3 Validation of the tangent linear model including cloud-radiation processes

3.1 Experimental framework

The accuracy of the linearization of described cloud and radiation parametrization schemes is studied with respect to pairs of non-linear results.

In the validation experiments, the difference between two non-linear integrations (one starting from a background field $\mathbf{x}^b$ and the other one starting from an analysis $\mathbf{x}^a$) is computed. This difference is then used as the standard reference of the tangent-linear integrations which propagate in time the analysis increments $\delta\mathbf{x} = \mathbf{x}^a - \mathbf{x}^b$ with the trajectory taken from the background field (Janisková *et al.* 1999, Mahfouf 1999).

The experiments have been produced by a T63L31 version of the ECMWF global spectral model. Three different situations, starting from 15 March 1999 at 12UTC, 15 June 1999 at 12UTC and 15 December 1998 at 12UTC with an integration up to 24 hours, have been studied. The results are evaluated for a 6-hour integration (the length of the current assimilation window), as well as for 12- and 24-hour integrations.

In the operational ECMWF model, the full radiation computations are presently done every 3 hours (every 1 hour during the firrst-guess forecasts used as part of the assimilation system or during the first 6 hours of any operational forecast). The computations are carried out on a reduced horizontal grid, corresponding to all points around the poles and decreasing to one point of four in the longitudinal direction in the tropics (J.-J. Morcrette, 2000). However, the assimilation of cloud properties will require calling the linearized radiation more often and at the full spatial resolution. This is why the radiation and cloud schemes have been used at each time step and in every grid points in our experiments.

For a quantitative evaluation of the impact of the cloud and radiation schemes, their relative importance is evaluated using mean absolute errors between tangent-linear and non-linear integrations as

$$\varepsilon = \overline{\left|[M(\mathbf{x}_{an}) - M(\mathbf{x}_{fg})] - M'(\mathbf{x}_{an} - \mathbf{x}_{fg})\right|} \tag{15}$$

where M is the forecast model starting from different initial conditions:
$\mathbf{x}_{an}$ - from analysis,
$\mathbf{x}_{fg}$ - from the first guess,
M' is the tangent-linear model starting from the initial conditions $(\mathbf{x}_{an} - \mathbf{x}_{fg})$,
$\overline{(...)}$ represents the mean over a particular domain.

As a reference for the comparisons, an absolute mean error for the tangent-linear model without radiation ε_{ref} is taken. ε_i is defined as absolute mean error for version i of the tangent-linear model with the different schemes included with respect to pairs of non-linear integrations with the full physics. Then an improvement coming from including more physics in the tangent-linear model can be expressed as

$$\varepsilon_i < \varepsilon_{ref} \tag{16}$$

Global zonal mean errors as well as zonal mean errors for North20 (20N - 90N), South20 (20S - 90S) and Tropics (20N - 20S) separately have been evaluated. For clarity, the vertical profiles of absolute mean errors have been computed as well.

It is assumed that the radiation directly influences temperature field and as a consequence of temperature changes one could observe the impact of radiation on other quantities. This is

why, results are mostly presented for temperature perturbations, though during the validation, the results from other fields have been compared as well.

The following set of experiments for all situations have been run using the tangent linear model:

- without any radiation (reference run),
- with simplified linearized longwave radiation scheme,
- with shortwave radiation and simplified longwave radiation:
  - for clear sky,
  - using diagnostic cloud scheme,
- with shortwave and the more sophisticated longwave radiation schemes described in section 2.2:
  - for clear sky,
  - including diagnostic cloud scheme without any treatment of the thresholds,
  - using simplified diagnostic scheme with zero perturbation of the main part of the stratiform cloudiness (equation 12).

3.2 Solving threshold problems in the diagnostic cloud scheme

Including more physical processes to the linearized set of physics should lead to an improvement of the representation of the general feedbacks between the processes. This should then improve the fit of the tangent-linear model to non-linear one. However, one must be careful with non-linearities and discontinuities by which the physical processes are characterized. Without treatment of the most serious threshold processes, tangent-linear model can turn to be inadequate.

A detailed investigation of the proposed radiation and diagnostic cloud schemes has shown a problem coming from the cloud parametrization. Although the cloud scheme together with radiation did not lead to any occurence of spurious perturbations (see results in section 3.3 Experimental results, especially in subsection 3.3.5 Singular vectors with new schemes), it degraded results. The problem was not so serious when cloudiness was only used with shortwave radiation. A one-dimensional version of the cloud and radiation schemes has been used to study the accuracy of the tangent-linear approximation for the radiative fluxes. When applied to a number of atmospheric profiles, some enlarged perturbations compared to the finite differences have been identified. The results of the tangent-linear approximation for the shortwave heating rates computed using the new radiation with the diagnostic cloud scheme and compared with the finite differences are presented in Fig. 2. One can see unrealistic perturbations (responsible for very bad tangent-linear approximation) obtained when using the linearized schemes (Fig. 2a). The proposed modification (described below in this section) improved the results significantly (Fig. 2b).

A careful look at the problem has shown that this comes from the parametrization of cloudiness used as a function of relative humidity (eq. 12). An intermediate value of the function (before squaring it), the function itself and corresponding derivatives (using two different perturbations of input relative humidity as $0.1RH_e$ and $0.2RH_e$) are presented in Fig. 1. The function is very steep in order to parametrize the growth of the cloudiness from 0 to 1 in quite narrow interval of relative humidity starting from the threshold value characterized by constant b. From a differentiation of the intermediate function (thick solid line in Fig. 1)

$$f_{int} = \frac{RH_e - b}{1 - b} = \frac{RH_e}{1 - b} - \frac{b}{1 - b} \tag{17}$$

one obtains

$$df_{int} = \frac{dRH_e}{1 - b} \tag{18}$$

Since the derivative of the constant is zero, the derived function misses the similar shift in vertical as in the case of original function. When $b = 0.8$, the shift of the function is equal to 4. The function actually starts from -4 for zero humidity and it grows up to 1 in the case of 100% relative humidity. The max-function is used to avoid unrealistic negative cloudiness and only positive or zero values are then used. The condition of max-function also restricts the derivative to be non-zero in the same interval (dashed parts of the lines in Fig. 1 represents the function in the whole interval of relative humidity without applying max-function). The derivative is then characterized by a large jump at the threshold point b in order to reach the derived values of the function df_{int} (solid line with empty circles and triangles for $0.1RH_e$ and $0.2RH_e$, respectively). Afterwards using the square of such function creates a state when the derived function can produce larger values than the function itself for certain values of relative humidity (solid line with filled circles and triangles for $0.1RH_e$ and $0.2RH_e$, respectively). Due to the described steep function necessary for parametrizing the dependency of cloudiness directly on relative humidity, we have failed to find any its suitable regularization.

Another problem is the occurence of positive relative humidity perturbations close to the saturation. This is quite realistic situation in the atmospheric processes. However, if used in the cloud scheme this will create a situation, when adding a positive cloudiness perturbation to the cloudiness close to one, would exceed this value. In the atmosphere, increasing humidity in the case of fully covered sky will increase cloud liquid water. The simple diagnostic cloud scheme is not able to treat such situation. In order to avoid both problems, it was decided to set the derivative of the function of relative humidity to zero. This also means that the high level cloud cover is then constant in the particular time step. Middle level and low level clouds are only modified by a linear transition up to weak ascent using vertical velocity. In such a way, the tangent-linear model has been simplified by accounting for only part of linearization. Liquid water and ice water can however be modified by temperature perturbations. The results presented in Fig. 2b and in section 3.2 justify this choice.

3.3 Experimental results

3.3.1 Zonal mean diagnostics

The impact of including new radiation and cloudiness schemes into existing set of linearized physics has been evaluated using the zonal mean diagnostics of mean absolute errors as described in section 3.

Such diagnostic has been run for all the situations. To illustrate the general features of the impact, Fig. 3 presents results for the situation of 15 March 1999 12 UTC and for 24-hour forecast. All other results of zonal mean diagnostic are then summarized in Tables 1 - 3. They are presented in the percentage of an improvement (-), resp. worsening (+) of investigated tangent linear model with respect to the tangent-linear model without any radiation. The minus sign means that the absolute errors ε of investigated tangent-linear integration are reduced. Fig. 3a shows the error differences (in terms of fit to the nonlinear model with the full physics) between the tangent-linear (TL) model including current linearized longwave radiation scheme and the TL model without any radiation. Fig. 3b and 3c present the same differences, but using the TL model including the new radiation scheme with simplified cloudiness (described in section 3.1) and for clear sky, respectively.

One can see that the current longwave radiation scheme (Fig. 3a) only gives a slight global improvement of 0.31%. Negative impacts appear in the middle of atmosphere, especially in the northern hemisphere over 70N and in the southern one over 80S. In those areas, the tangent-linear model without any radiation appears to be a better approximation of the full non-linear model. The problems come from over-simplifications of the linearized longwave radiation scheme, which uses the constant emissivity approach which is not appropriate in the stratosphere (Mahfouf, 1999).

Using tne new longwave and shortwave radiation schemes together with cloudiness (Fig. 3b) gives the global improvement of 4.71%. Some small worsening of the results are observed on few places in the northern hemisphere. They are slightly more significant in the southern hemisphere. Overall, a positive impact is noticed close to the surface and in the tropics. When the radiation is run without cloudiness in the TL model (Fig. 3c), the improvement is only slightly smaller (4.69%). It means that the impact of the diagnostic cloud scheme used with radiation is small.

Table 1 summarizes the results of relative comparisons for 6-, 12- and 24-hour integration of the March situation and for North20, South20, Tropics as well as globally. The results for 24-hour integration of the June and December situations are in Tables 2 and 3, respectively. The tables contain results from all different experiments which have been run and described above.

The largest improvement is achieved when using both shortwave and more sophisticated longwave radiation ('new lw'). When the linearized cloud scheme is used without any modification

(as described in subsection 3.2), the results are worse than those obtained for clear sky conditions. This corroborates the need for such modification. Even applying the modification, the results are slightly better, except in the Tropics, for the clear sky radiation than for the radiation with clouds. In the Tropics, cloudiness has a positive impact when used in the linearized model. The results are situation dependent. The worst results (however still leading to an improvement after 24-hour integration, except South20) were obtained for the June situation (Table 2). Actually, this was a situation when any radiation scheme did not improve the results significantly. For the December situation, the simplified linearized longwave radiation scheme is worsening the results over North20, which is not the case anymore for new radiation.

One can see that including more sophisticated radiation schemes gives a general improvement in the Tropics and a large reduction of the errors as well as a reduction of some existing negative impacts for longer integrations. The impact of using cloudiness with the radiation is not as large as one would expect and not always positive. The negative impacts are possibly a consequence of introducing more non-linearities in the linearized physics with cloud processes. This will require further investigations.

3.3.2 Impact of including new schemes on the vertical profiles

In order to make a relative comparison between the different experiments, the mean values of $\varepsilon_i - \varepsilon_{ref}$ (see equations 15, 16) have been computed for the different domains (North20, South20 and Tropics). The vertical profiles of the mean values are presented in Fig. 4, 5 and 6 for temperature, u-wind component and specific humidity, respectively. The results for 6-hour integration are on the left column and those ones for 24-hour integration are on the right column. The comparisons are displayed for the simplified longwave radiation scheme (dashed line) as well as for the new radiation (longwave and shortwave) with simplified cloud scheme (solid line) and for clear sky (dot-dashed line).

By comparing impact of the schemes on temperature (Fig. 4), one can see reduced errors, especially close to the surface and in the lower troposphere in the 6-hour integration for all evaluated domains when including any radiation to the linearized physics. However, the reduction is larger for the new radiation scheme. In this case, an improvement is observed through the whole vertical profile in North20, on most levels in South20 (except levels between 900 and 650 hPa) and up to the middle troposphere in the Tropics (in higher levels, the results are as positive as negative). One can see that the old radiation scheme improves the results in the lower troposphere and degrades them for higher levels. After 24 hours of integration, the results are much more in favour of the new radiation scheme which improves the fit of the tangent-linear model to the nonlinear one through the whole vertical profile for North20 and Tropics. It is also the case for South20, except levels between 900 and 700 hPa. Adding the cloudiness scheme to the radiation has a very small impact and except in the tropics is mainly negative.

One can wonder whether the improvements justify the additional effort to develop the code and

the additional computer time. However, the differences are not really small as they represent up to 10% of the perturbation value. Furthermore, the displayed values are mean values for a big domain. In specific situations (as presented in section 3.2.4), the differences can represent several Kelvins.

The results for u-wind component are displayed in Fig. 5. An improvement coming from the new radiation scheme is observed nearly through the whole vertical profiles for all domains in the 24-hour integration. For the 6-hour integration, it is also the case for North20, lower troposphere of South20 and for the Tropics up to 200 hPa. The impact of the old radiation scheme on u-wind is negligible and it is mainly negative for 6-hour integration and the upper part of the atmosphere. A positive impact of using cloudiness together with the radiation is seen especially in the Tropics.

Except for the levels close to the surface, including a new radiation scheme in the linearized physics leads to worse results for specific humidity in the 6-hour integration (Fig. 6). This is a little suprising as one can see an improvement for temperature. It is possible that due to the interactions of radiation with the simplified moist physical processes, longer integration period is necessary for establishing a proper equilibrium. Indeed, the results are improved for 24-hour integration close to the surface and in the lower troposphere. The impact is only slightly negative elsewhere. The largest improvement is observed in the lower and middle troposphere of the tropics. The old radiation scheme has only a slight influence on specific humidity. It often improves or worsens the results at the same levels as the new radiation scheme, but the magnitude of the impact of the old radiation schemes is always smaller.

The relative comparison between the different tangent-linear models have shown a general improvement in the lowest model levels when the new radiation and cloud schemes are used. The results are also better for the tropics suggesting that a proper balance between shortwave, longwave radiation and moist processes is crucial. A positive impact coming from the new radiation is amplified and the negative one (if any) is reduced for longer integration times.

Our experimentation raises the question, why the impact of the cloud scheme used with the radiation scheme is so small. To get an answer, some special experiments have been performed and results are presented in the following section.

3.3.3 Investigation of cloudiness impact used in the radiation scheme

To answer the question about the impact of cloudiness used with the radiation scheme comparisons have been done between absolute mean values of:

$$| TL_{\text{clear sky}} - TL_{\text{cloudiness}} | \text{ and } | FD_{\text{clear sky}} - FD_{\text{cloudiness}} |,$$

where TL stands for the tangent-linear model and FD for the finite differences.

The results of such comparison are displayed in Fig. 7 for temperature (a) and for specific humidity (b). One can see that the impact of the cloudiness in the TL model (full line) is in-

deed much smaller than for FD (dot-dashed line). Since there is a simplification for convective cloudiness in the TL model (no perturbation of convective precipitation due to the simplified convective scheme), an experiment has been run without taking into account convective cloudiness in the non-linear model (long-dashed line) and in the TL model (dashed line) as well. In this case, the impact of the cloudiness in the TL model is larger with more vertical structures (especially for specific humidity). However, it is still smaller than in FD. Since one could observe some improvement in TL approximation when convective cloudiness is not used, another experiment has been done using the trajectory with complete full physics and the TL model without convective cloudiness (dotted line). The results are better than those ones from the original experiment (with both, stratiform and convective types of cloudiness), though not yet satisfactory either. An improvement is coming probably from the fact that the approximation, having only trajectory of convective precipitation and no perturbation, is not good enough. In this approach, one allows the modification of relative humidity trajectory due to the convective precipitation without any modification of relative humidity perturbation. Such inconsistently modified humidity is then entering to the computation of stratiform cloudiness. It seems that a better approach for the simplification of the diagnostic cloud scheme (however physically less realistic) is not to take into account convective cloudiness in the TL model at all. All supersaturation is then released to the stratiform clouds. The described cloudiness sensitivity study suggests that properly parametrized convective clouds may have a really important effect in the linearized model. As it was mentioned, we aim at having a linearized simplified prognostic cloud scheme where the convective cloudiness does not depend explicitly on convective precipitation. A better coupling of the cloudiness scheme with convective processes will also require a more comprehensive linearized convection scheme.

3.3.4 Case study for the situation of 15 December 1998

The previous sections described the quantitative impact of adding new radiation schemes to the existing set of linearized physics. Diagnostics were performed in terms of mean absolute errors. It was mentioned that improvement coming from the new radiation and the diagnostic cloud scheme may look small in terms of mean values. However, the differences can be quite large for some situations. During the validation of the tangent-linear approximation of the linearized physics with new schemes, several cases with significant differences (several Kelvins for temperature) between the tangent-linear and the finite difference integrations have been observed. One of such cases is presented in this section.

Fig. 8 shows a meteorological description of the situation 15 December 1998 18UTC over the area of Turkey. 6-hour forecast of low level cloud cover (starting from 15 December 1998 at 12UTC) and 6-hour cumulative large scale and convective precipitation are presented in Fig. 8a and 8b, respectively. The nonlinear forecast is run from the background initial field as the trajectory has been taken from the background field in our experiments. The situation is characterized by low cloud cover up to around 60 % and around 1 mm of precipitation amount during 6 hours in the area of our interest. As it was mentioned at the beginning of section 3, the difference between two non-linear integrations (one starting from a backgroung field (FG) and

the other one starting from analysis (AN) are used as the standard reference of the tangent-linear integrations). Fig. 8c and 8d present the differences between two non-linear integrations in low cloud cover and cumulative precipitation, respectively. Positive differences in the precipitation field over Turkey means (comparing with Fig. 8b) that the precipitation produced by the forecast from AN was negligible compared to FG forecast. The described situation is such that when using a radiation scheme taking into account humidity and cloudiness the results should be improved with respect to the simplified longwave radiation scheme.

Fig. 9 shows the 6-hour evolution of temperature increments at level 31 (the model level closest to the surface in our experiments) produced from the differences between two non-linear forecasts (Fig. 9a) and from the different tangent-linear integrations (Fig. 9b-f). Fig. 9b displays the temperature perturbation using the TL model without any radiation. One can see a strong positive temperature increment of 2.89 K over Turkey, which only reaches 0.5 K in the case of the finite differences. Including the simplified longwave radiation scheme (Fig. 9c) makes the situation even worse since it increases the perturbation up to 3.28 K. When the shortwave radiation scheme (Fig. 9d) is included on top of the old longwave scheme, the perturbation is decreased to 0.93 K. Replacing the old longwave radiation scheme (Fig. 9e) by the more sophisticated one (described in section 2.2) brings further reduction up to 0.46 K. In this case, the tangent-linear results correspond much better to the finite differences. Fig. 9f displays the results obtained with the new radiation scheme in clear sky conditions. The temperature increments in this case are close to the ones produced using the cloud scheme with radiation. It is important to realize that the radiation scheme run in clear sky conditions contains information about humidity perturbations (used in the computation of absorber amounts).

The above situation is a daytime period when both radiation schemes (shortwave and longwave) play an important role during the whole 6-hour integration. Both schemes are required in the tangent-linear model in order to get temperature increments which are in better agreement with the finite differences.

To investigate this situation over the whole vertical profile, a cross-section was drawn through the centre of maximum temperature increments. Such vertical profiles for the finite differences and the tangent-linear approximations are presented in Fig. 10a-f. One can see that the main differences between the various tangent-linear evolutions and the finite differences appear close to the surface and in the planetary boundary layer. The impact of cloudiness used with the radiation scheme is more obvious in the vertical profile. The positive temperature increments over the domain of interest (between 25E and 45E), when using cloudiness, correspond better to the finite differences than for the clear sky radiation run. Patterns are more similar to those obtained in the nonlinear run.

The described example shows the importance of using a more sophisticated radiation scheme which can lead to significant modifications of the increments in certain situations.

3.3.5 Singular vectors with the new schemes

Singular vectors with the linearized physics including the new radiation and cloudiness parametrization schemes has been computed. The usefulness of singular vectors to identify non-meteorological instabilities produced by the linearized physics was illustrated for the ECMWF model by Mahfouf (1999). Since some worsening of the results (in terms of the perturbation evolution) has been identified when using the linearized cloud scheme (before applying the modification described in section 3.2) with radiation, we used this technique to find out whether the new schemes can produce spurious unstable modes.

Singular vectors have been computed north of 30N over a 48-hour optimization period starting from 15 March 1999 at 12UTC with a T42L31 linearized model. The different versions of the linearized model presented in the previous sections have been used. The adiabatic model with the simple vertical diffusion scheme (Buizza, 1994) used in the ECMWF EPS (adiab-svd) and the model with improved linearized physics (Mahfouf, 1999) used in the operational 4D-Var (oper) have been taken as references for the comparisons. Then two runs with the new radiation and cloudiness schemes have been investigated - one with linearized cloudiness without any modification (new rad+cloud1) and another one taking into account only part of the linearization for cloudiness as described in section 3.1.

The total energy amplification of the first 20 evolved singular vectors for the described runs is compared in Fig. 11. The amplification factors are defined as the square root of the ratio between the total energy norm at optimization time and at initial time. These factors obtained with the non-modified cloud scheme and the cloud scheme using zero perturbation of the main part of the stratiform cloudiness (the cloudiness is not modified by changing relative humidity in particular time step) look very similar. These two runs present more differences with the improved linearized physics. The inclusion of the new radiation produces slightly smaller growth rates.

The vertical profile of total energy at final time averaged over the first 20 singular vectors is presented in Fig. 12. One can see again high similarity of two different runs with the new radiation scheme. The effect of including new radiation is to reduce total energy up to 250 hPa with the most significant effect between 600 and 900 hPa. The maximum of energy at final time is located in the upper troposphere as presented by Buizza (1994) and Mahfouf (1999). No large unrealistic amplification rates have been identified with the new schemes.

The possible differences between the singular vectors computed using the different linearized models can be quantified by determining a similarity index as in Buizza (1994). The indices are computed by projecting one set of the singular vectors onto another one. The mean of the projection coefficients is a measure of how much the two sets of the singular vectors differ. The index 0 represents orthogonal subspaces and index 1 means that the subspaces are identical. The results for the March situation are presented in Table 4. The high similarity between the runs with the new radiation schemes is obvious which is consistent with all other comparisons. Including the new radiation scheme into improved linearized physics leads to slightly different

structures as indicated by the smaller similarity index between 'new rad' runs and 'oper' ones. However, this similarity is higher than in the comparison of 'new rad' and 'oper' runs against 'adiabsvd'.

Using the singular vectors with new radiation and cloudiness schemes does not lead to identification of any extreme growth rates. It also showed high similarity between using the non-modified cloud scheme and the modified one (using only part of the linearization), while later leads to improvement of the results in terms of perturbation evolutions. This similarity indicates that the impact of the diagnostic cloud scheme with the radiation scheme is small.

4 Conclusion

The linearized versions (tangent-linear and adjoint) of the ECMWF shortwave radiation have been developed without a priori modifications. A strategy combining neural networks and Jacobian matrices has been defined for the linearized longwave radiation scheme. For the time being, a diagnostic cloud scheme has been linearized to be used with radiation.

The accuracy of the linearization of both the radiation and diagnostic cloud schemes has been examined by comparing the evolution over 24 hours of a perturbation (of the order of magnitude of analysis increments) with the tangent-linear model and the finite difference between two nonlinear forecasts using full physics (one from a basic state and the other one from a perturbed state). The results obtained suggest that the inclusion of a more sophisticated radiation package to existing linearized physical parametrizations improves the fit to the nonlinear model. Singular vector computation shows that the inclusion of the new radiation schemes produces slightly smaller growth rates, but otherwise no highly unstable modes have been identified. This suggests that the new schemes describe meteorological features and their inclusion to the existing linearized set of simplified physics should not lead to spurious perturbations.

All the tests have shown that the impact of the linearized diagnostic cloud scheme is very small. This will require a future revisiting of the cloudiness parametrization for the linearized model. The development of a simplified linearized prognostic cloud scheme will be undertaken in the near future. Such development is necessary for improving cloud-radiation interactions and to improve the coupling with the convection scheme. This will also require a revision of the linearized mass-flux convection scheme.

In the future, feasibility studies in a 1D-Var framework will be performed using cloudy radiances from operational satellites (TOVS/ATOVS, Meteosat, SSM/I). Cloud profiles (fractional cover, water and ice contents) will be adjusted to improve simulated radiances. Appropriate background errors will have to be defined for these variables. When a linearized prognostic cloud scheme is available both thermodynamical (temperature, humidity) and dynamical (vertical velocity) variables will be adjusted in the variational problem. The importance of cloud profile

observations together with radiative measurements will be assessed using field experiment data sets (ARM, CLARE).

References

Buizza, R. , 1994: Impact of simple vertical diffusion and of the optimisation time on optimal unstable structures. *ECMWF Technical Memorandum*, **238**, 54 pp.

Chéruy, F., Chevallier, F., Morcrette, J.-J., Scott, N.A. and Chédin, A. ,1996: Une méthode utilisant les techniques neuronales pour le calcul rapide de la distribution verticale du bilan radiatif termique terrestre. *C. R. Acad. Sci. Paris*, **322: IIb**, 847-873.

Chevallier, F., Chéruy, F., Scott, N.A. and Chédin, A. , 1998: A neural network approach for a fast and accurate computation of longwave radiation budget. *J. Appl. Meteor.*, **37**, 1385-1397.

Chevallier, F., Morcrette, J.-J., Chéruy, F. and Scott, N.A. , 2000: Use of a neural network-based longwave radiative transfer scheme in the ECMWF atmospheric model. *Q. J. R. Meteor. Soc.*,**126**, 761-776.

Chou, C. and Neelin, J.D. , 1996: Linearization of longwave radiation scheme for intermediate tropical atmospheric model. *J. Geophys. Res.*, **101D**, 15129-15146.

Ebert, E.E. and Curry, J.A. , 1992: A parametrization of ice optical properties for climate models. *J. Geophys. Res.*, **97D**, 3831-3836.

Eyre, J.R. , 1995: Variational assimilation of remotely-sensed observation of the atmosphere. *ECMWF Technical Memorandum*, **221**, 14 pp.

Fouquart, Y. , 1987: Radiative transfer in climate models. *Physically Based Modelling and Simulation of Climate and Climatic Changes*, M.E. Schlesinger, Ed., Kluwer Acad. Publ., 223-284.

Fouquart, Y. and Bonnel, B. , 1980: Computations of solar heating of the earth's atmosphere: a new parametrization. *Beitr. Phys. Atmosph.*, **53**, 35-62.

Janisková, M., Thépaut, J.-N. and Geleyn, J.-F. , 1999: Simplified and regular physical parametrizations for incremental four-dimensional variational assimilation. *Mon. Wea. Rev.*, **127**, 26-45.

Mahfouf, J.-F. , 1999: Influence of physical processes on the tangent-linear approximation. *Tellus*, **51A**, 147-166.

Mahfouf, J.-F., Beljaars, A., Chevallier, F., Gregory, D., Jakob, C., Janisková, M., Morcrette, J.-J., Teixeira, J. and Viterbo, P. , 1999: The importance of the Earth Radiation Mission for numerical weather prediction. *ECMWF Technical Memorandum*, **288**, 77 pp.

Mahfouf, J.-F. and Rabier, F. , 2000: The ECMWF operational implementation of four-dimensional variational assimilation. Part II: Experimental results with improved physics. *Quart. J. Roy. Meteor. Soc.*, in press.

Marécal, V. and Mahfouf, J.-F. , 2000: Variational retrieval of temperature and humidity profiles from TRMM precipitation data. *Mon. Wea. Rev.*, accepted for publication.

Morcrette, J.-J., Smith, L. and Fouquart, Y. , 1986: Pressure and temperature dependence of absorption in longwave radiation parametrizations. *Beitr. Phys. Atmos.*, **59**, 455-469.

Morcrette, J.-J. , 1989: Description of the radiation scheme in the ECMWF operational weather forecast model. *Research Department Tech. Memo*, **165**, 26 pp.

Morcrette, J.-J. , 1990: Impact of changes in the radiation transfer parametrization plus cloud optical properties in the ECMWF model. *Mon. Wea. Rev.*, **113**, 847-873.

Morcrette, J.-J. , 1991: Radiation and cloud radiative properties in the ECMWF operational forecast model. *J. Geophys. Res.*, **96D**, 9121-9132.

Morcrette, J.-J. , 2000: On the effects of the temporal and spatial sampling of radiation fields on the ECMWF forecasts and analyses. *Mon. Wea. Rev.*, **128**, 876-887.

Rabier, F., Järvinen, H., Klinker, E., Mahfouf, J.-F. and Simmons, A. , 2000: The ECMWF operational implementation of four-dimensional variational assimilation. Part I: Experimental results with simplified physics. *Quart. J. Roy. Meteor. Soc.*, in press.

Park, S.K. and Droegemeier, K.,K. , 1997: Validity of the tangent linear approximation in moist convective cloud model. *Mon. Wea. Rev.*, **125**, 3320-3340.

Slingo, J.M. , 1987: The development and verification of cloud prediction scheme in the ECMWF model. *Quart. J. Roy. Meteor. Soc.*, **113**, 899-927.

Tiedtke, M. , 1993: Representation of clouds in large-scale models. *Mon. Wea. Rev.*, **121**, 3040-3061.

Verlinde, J. and Cotton, W.R. , 1993: Fitting microphysical observations of nonsteady convective clouds to a numerical model: An application of the adjoint technique of data assimilation to a kinematic model. *Mon. Wea. Rev.*, **121**, 2776-2793.

Washington, W.M. and Williamson, D.L. , 1997: A description of the NCAR GCMs. "GCMs of the atmosphere." J. Chang, Ed., *Methods in computational physics*, Vol.**17**, Academic Press, 111-172.

6-hour integration

	radiation scheme					
Domain	old radiation	old lw+new sw clear sky	old lw+new sw cloudiness	new sw+new lw clear sky	new lw+new sw cloud.	new lw+new sw zero pert.
global	-0.02%	-1.10%	-1.22%	-1.77%	-0.69%	-1.65%
Tropics	-0.48%	-1.47%	-1.84%	-1.40%	-0.62%	-1.51%
North20	+0.65%	-0.92%	-0.70%	-2.43%	-1.38%	-2.29%
South20	-0.04%	-0.71%	-0.81%	-1.65%	-0.08%	-1.19%

12-hour integration

	radiation scheme					
Domain	old radiation	old lw+new sw clear sky	old lw+new sw cloudiness	new sw+new lw clear sky	new lw+new sw cloud.	new lw+new sw zero pert.
global	-0.15%	-1.31%	-1.44%	-2.32%	-1.45%	-2.12%
Tropics	-1.14%	-2.59%	-2.99%	-2.15%	-1.58%	-2.26%
North20	+0.92%	-0.63%	-0.53%	-3.11%	-2.14%	-2.88%
South20	+0.09%	-0.24%	-0.25%	-1.71%	-0.53%	-1.39%

24-hour integration

	radiation scheme					
Domain	old radiation	old lw+new sw clear sky	old lw+new sw cloudiness	new sw+new lw clear sky	new lw+new sw cloud.	new lw+new sw zero pert.
global	-0.31%	-3.13%	-3.16%	-4.69%	-4.06%	-4.71%
Tropics	-1.93%	-3.60%	-3.99%	-2.72%	-2.52%	-3.09%
North20	+1.19%	-4.54%	-4.13%	-8.06%	-7.26%	-7.96%
South20	-0.16%	-0.94%	-1.05%	-3.09%	-2.12%	-2.82%

Table 1: Percentage of an improvement(-)/worsening(+) of the TL model with some of the listted radiation schemes with respect to the TL model without any radiation scheme for 6-, 12- and 24-hour integration. (Initial date of the integration: 15 March 1999 12UTC.)

24-hour integration

	radiation scheme					
Domain	old radiation	old lw+new sw clear sky	old lw+new sw cloudiness	new sw+new lw clear sky	new lw+new sw cloud.	new lw+new sw zero pert.
global	-0.13%	+0.89%	+0.58%	-1.10%	+2.20%	-0.41%
Tropics	-0.58%	-0.63%	-0.97%	-0.70%	+1.22%	-0.88%
North20	+0.02%	+1.01%	+0.54%	-1.25%	+2.80%	-0.95%
South20	+0.25%	+2.51%	+2.41%	+0.38%	+2.65%	+0.74%

Table 2: Same as Table 1, but for 24-hour integration and initial date of the integration 15 June 1999 12UTC.

24-hour integration

	radiation scheme					
Domain	old radiation	old lw+new sw clear sky	old lw+new sw cloudiness	new sw+new lw clear sky	new lw+new sw cloud.	new lw+new sw zero pert.
global	-0.65%	-2.03%	-2.11%	-3.28%	-2.19%	-3.22%
Tropics	-1.39%	-3.06%	-3.34%	-2.10%	-1.75%	-2.31%
North20	+0.47%	+0.72%	+0.70%	-1.54%	-0.56%	-1.39%
South20	-1.03%	-3.89%	-3.83%	-6.55%	-4.51%	-6.29%

Table 3: Same as Table 2, but for initial date of the integration: 15 December 1998 12UTC.

15/03/1999	adiabsvd	oper	new rad+cloud1	new rad+cloud0
adiabsvd	1	0.82	0.84	0.85
oper		1	0.92	0.93
new rad+cloud1			1	0.98
new rad+cloud0				1

Table 4: Similarity indices between unstable subsapces spanned by 20 singular vectors for different configurations: 'adiabsvd' - adiabatic model with simple vertical diffusion, 'oper' - operational improved linearized physics, 'new rad+cloud1' - new radiation with non-modified cloud scheme included, 'new rad+cloud0' - new radiation scheme with zero perturbation of the main part of cloudiness.

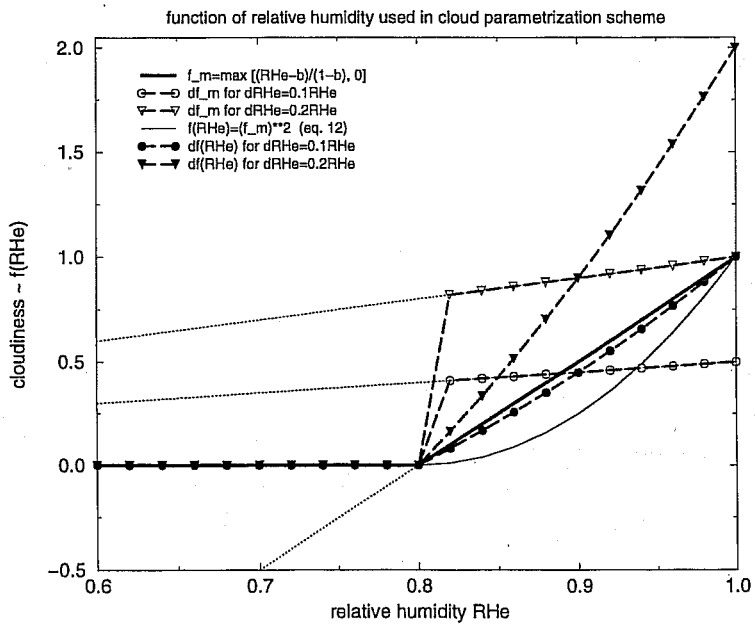

Figure 1: Intermediate function of relative humidity (before squaring it) used in cloud parametrization, the function $f(RH_e)$ itself and their corresponding derivatives using two different perturbations of input relative humidity as $0.1RH_e$ and $0.2RH_e$. The dotted part of the lines represents the function in the whole interval of relative humidity before applying max-function.

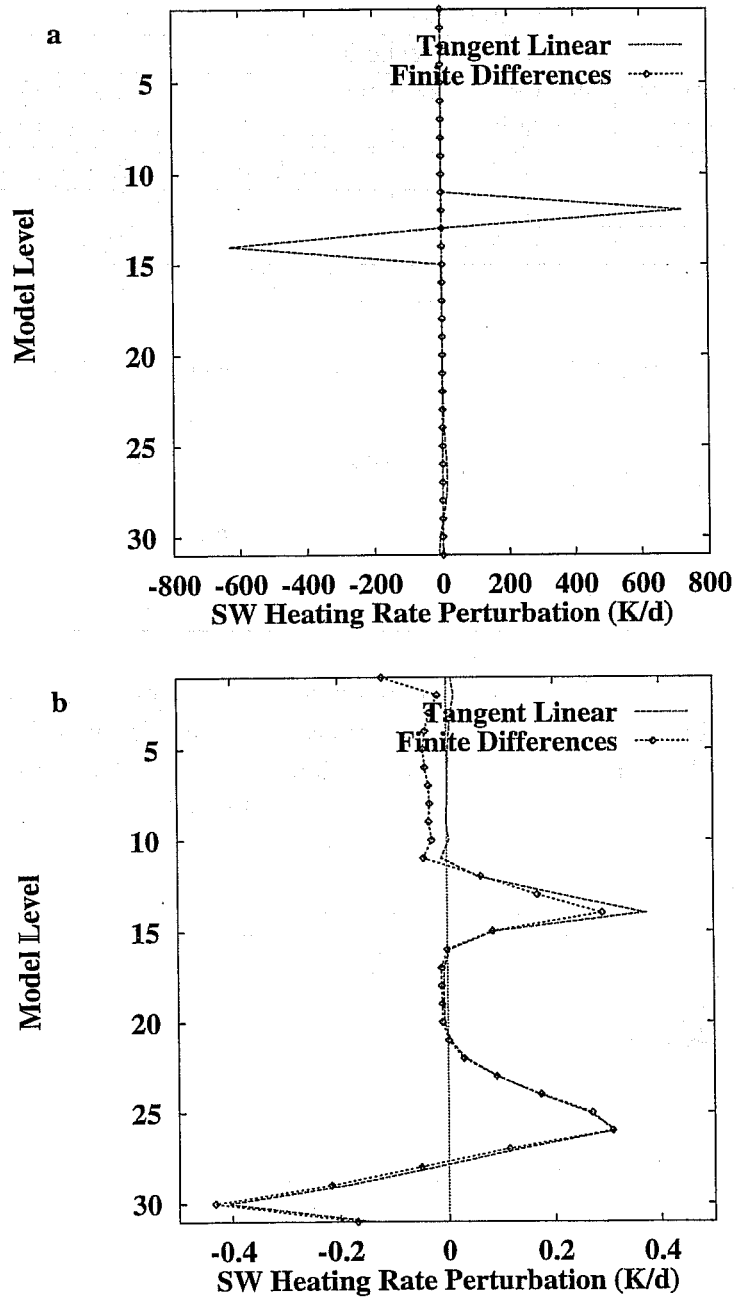

Figure 2: Comparison between the tangent-linear approximation for the shortwave heating rates (K/d) computed using the new radiation with the diagnostic cloud scheme and the finite differences. The upper pannel (a) shows the results without modification of the function of relative humidity used in the cloud scheme. The lower panel (b) displays the results after applying modification (as proposed in section 3.1)

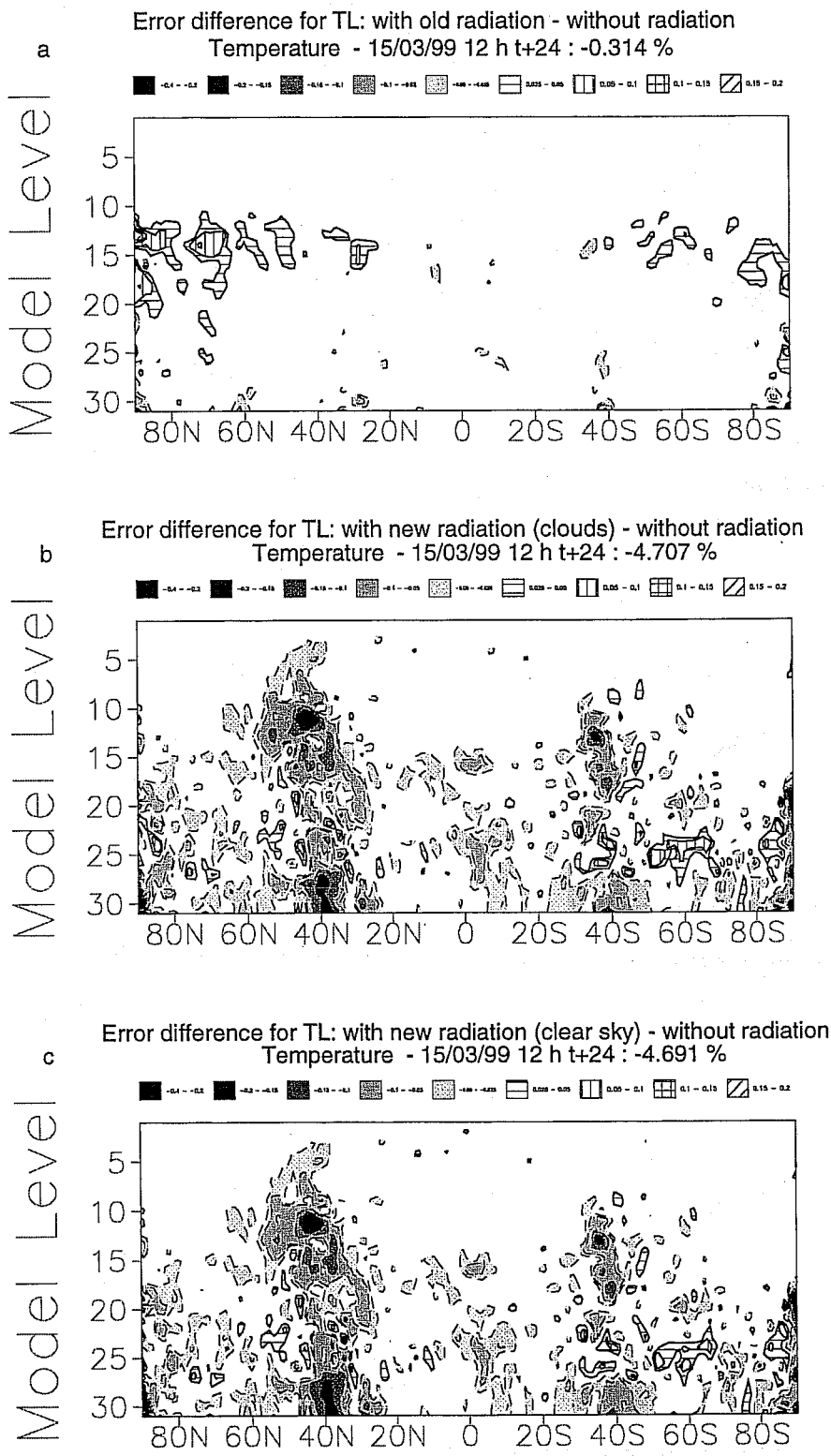

Figure 3: Influence of the different tangent-linear radiation schemes on the evolution of temperature increments presented as the error differences (in terms of fit to the nonlinear model with the full physics) between the tangent-linear (TL) model including currently used radiation scheme and the TL model without any radiation (a). (b) and (c) present the same, but using the TL model containing new radiation scheme with the simplified cloudiness and for clear sky, respectively. (24-hour forecast for the situation of 15 March 1999 12UTC, units: K)

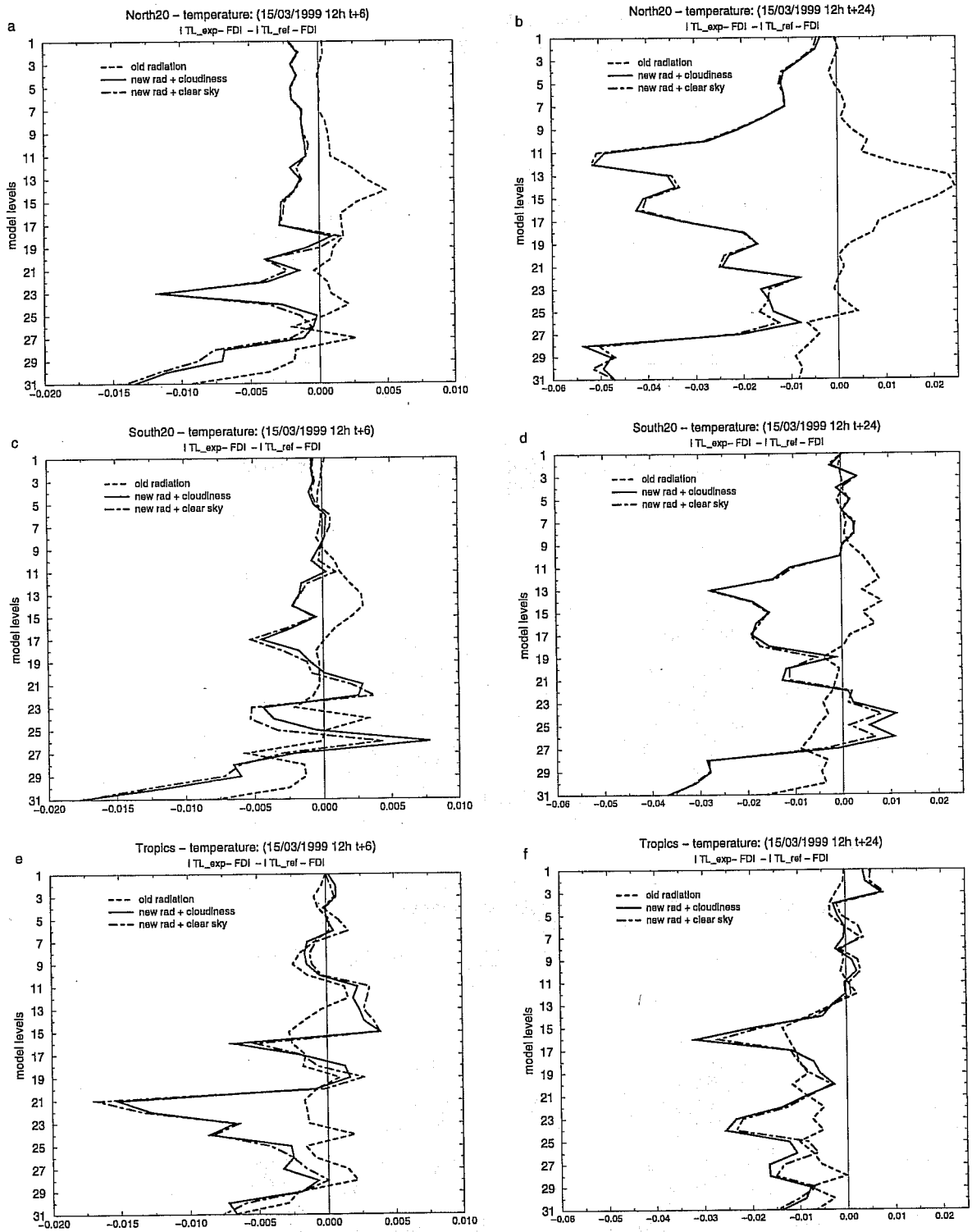

Figure 4: Vertical profiles of the mean values of error differences for temperature (units: K) from 6-hour (a,c,e) and 24-hour (b,d,f) integrations for North20 (a,b), South20 (c,d) and Tropics (e,f). The results are presented for currently used radiation scheme (dashed line) as well as for new radiation scheme with cloudiness (solid line) and for clear sky (dot-dashed line). Initial date of the integration: 15 March 1999 12UTC.

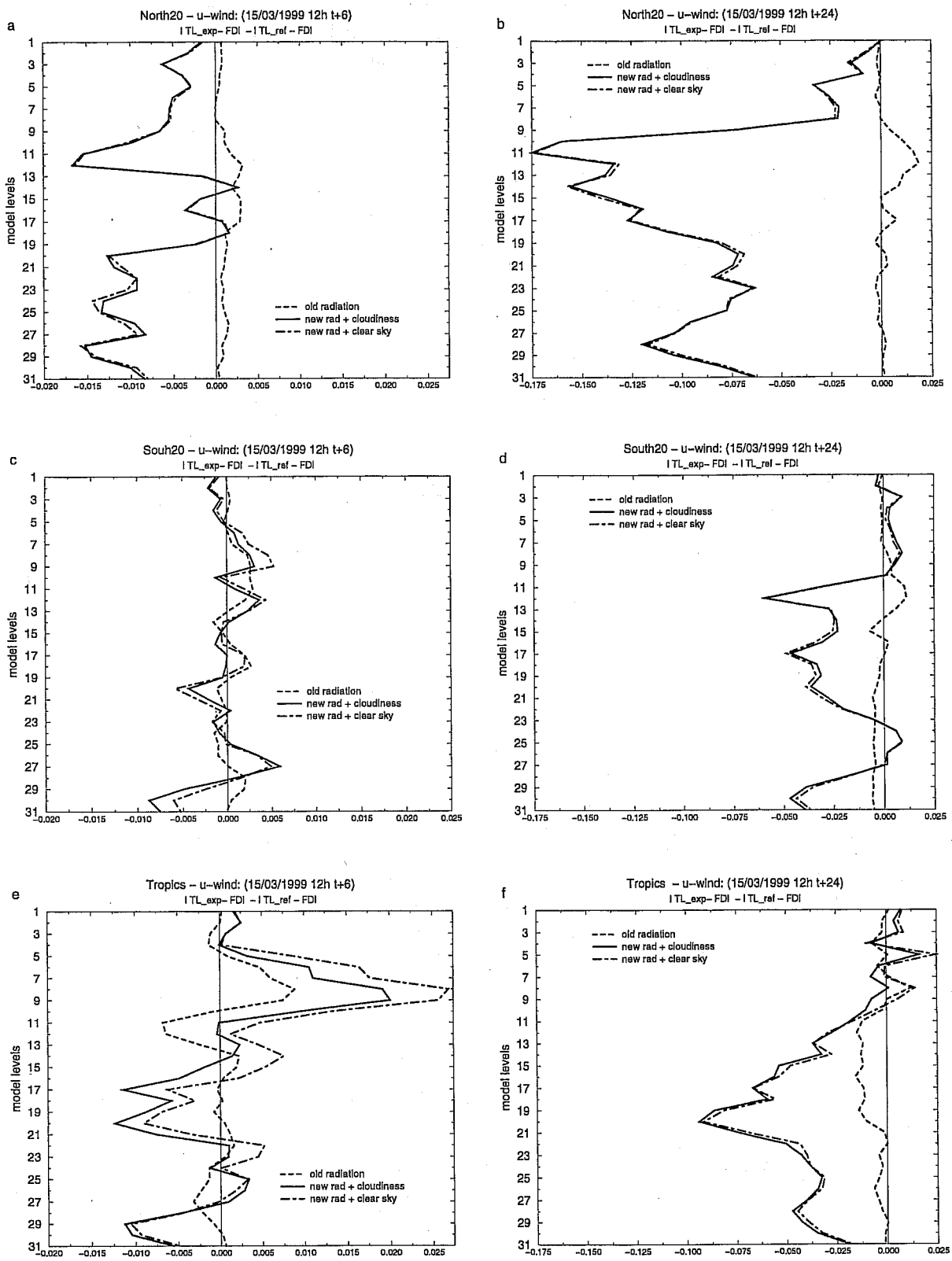

Figure 5: Same as Fig. 3, but for u-wind component (units: m s^{-1}).

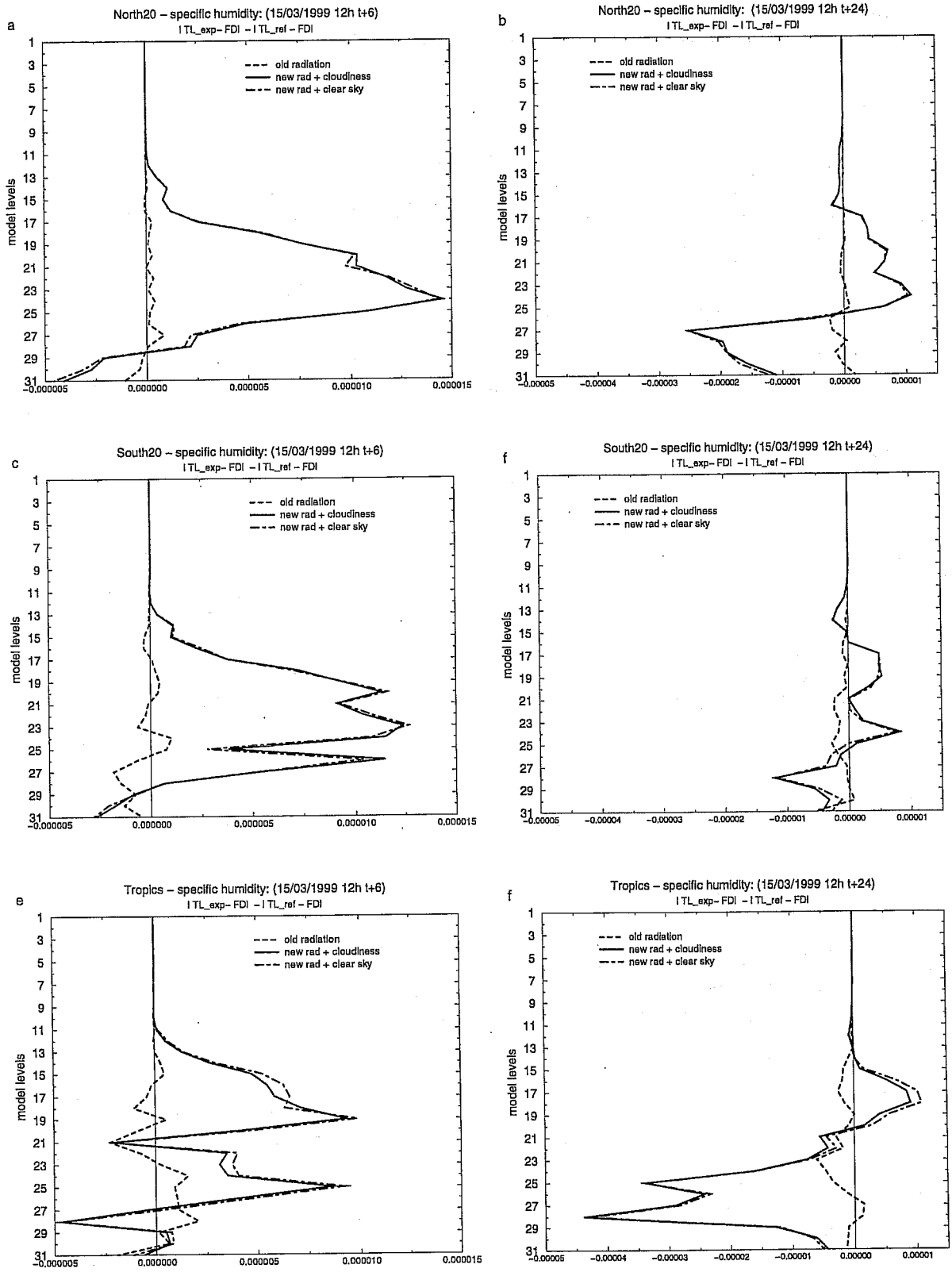

Figure 6: Same as Fig.3, but for specific humidity (units: kg kg^{-1}).

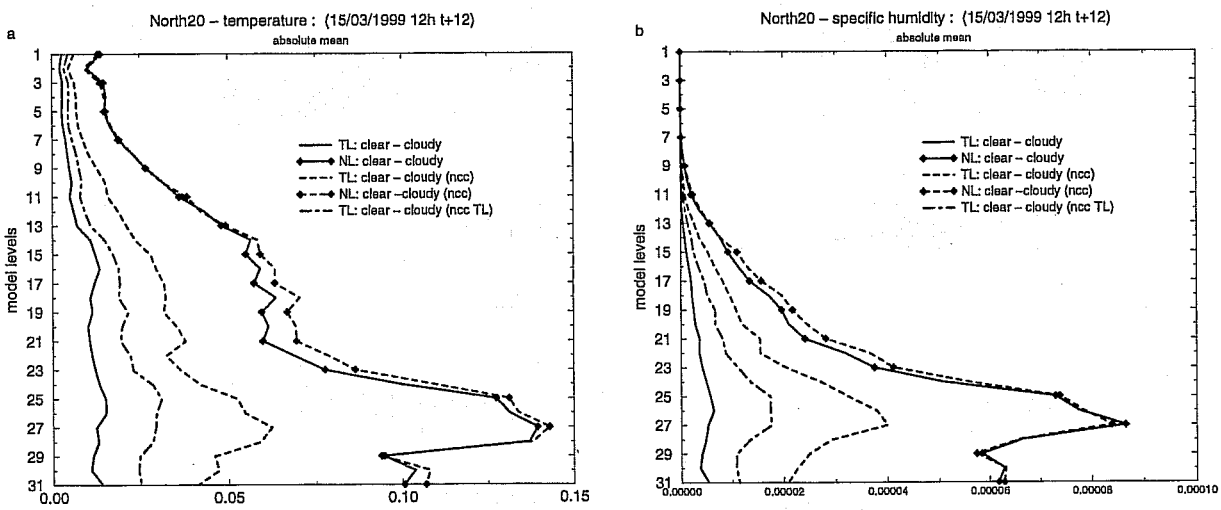

Figure 7: Impact of using cloudiness parametrization scheme with radiation one in the nonlinear model NL (lines with symbols) and in the tangent-linear model TL (lines without any symbol) for temperature (units: K) on the left (a) and specific humidity (units: kg kg^{-1}) on the right (b). The abbreviation 'ncc' means that no convective cloudiness is used neither in NL, nor in TL and 'ncc TL' means that the convective cloudiness is not used only in TL.

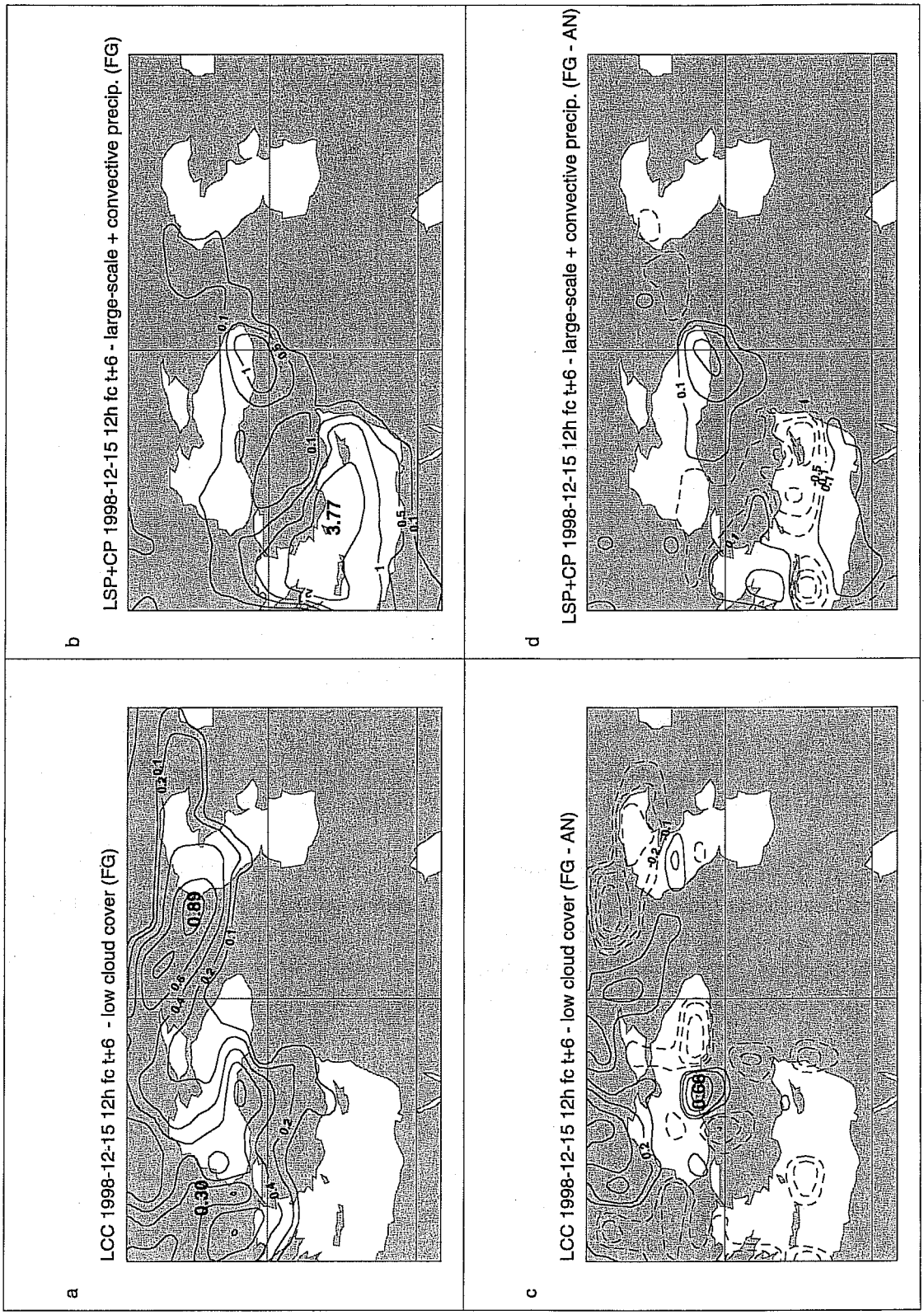

Figure 8: 6-hour forecat of low level cloud cover (a) and 6-hour cumulative large scale and convective precipitation (b) starting from the background initial field valid for 15 December 1998 at 12 UTC. The differences between two 6-hour nonlinear integrations, one starting from background field (FG) and the other one from analysis (AN) are also presented for low cloud cover (c) and for cumulative precipitation (d).

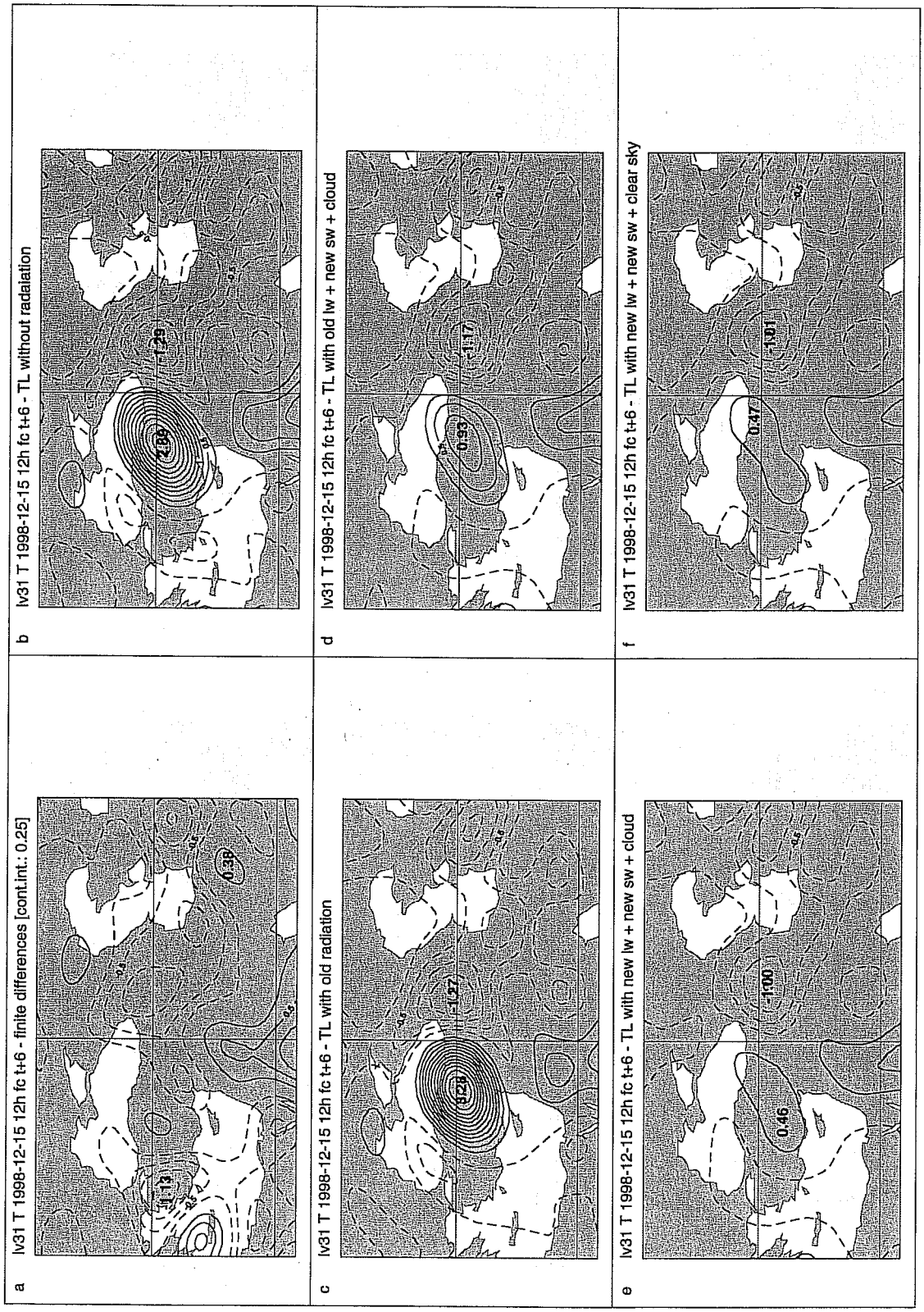

Figure 9: 6-hour evolution of temperature increments at level 31 (the closest model level to the surface) produced from the differences between two nonlinear forecasts (a) and from the different tangent-linear approximations (b-f) as displayed on the figure. Initial date of integration: 15 December 1998 12UTC.

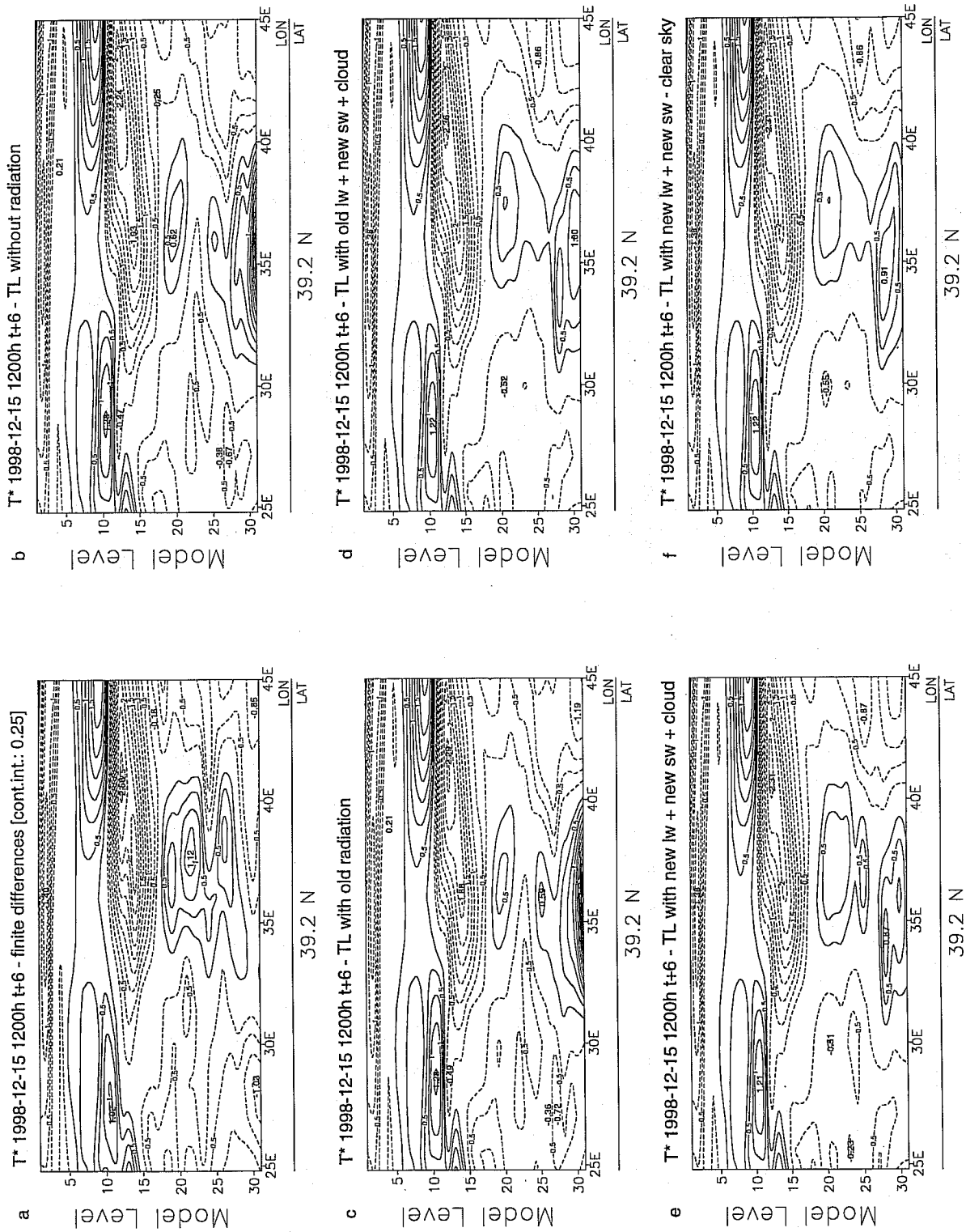

Figure 10: Same as Fig. 8, but for the vertical cross-section of temperature increments through the centre of their maximum values (latitude 39N and longitude 25E and 45E).

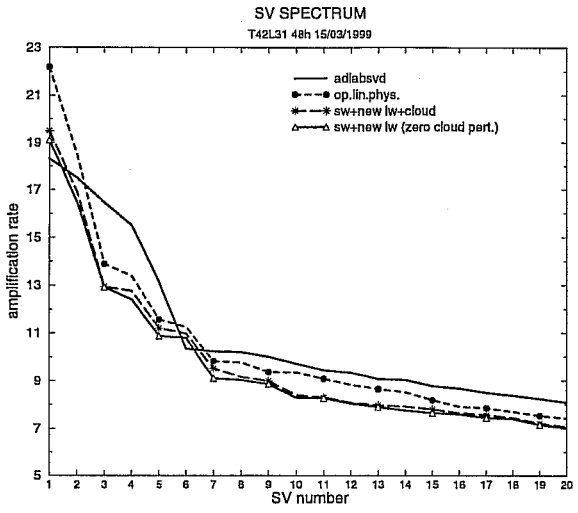

Figure 11: Total energy amplification of the singular vectors computed with a T42L31 linearized model using adiabatic model with simple vertical diffusion (solid line), operational linearized physics (dashed line with circles) and including new radiation scheme with non-modified cloud scheme (long-dashed line with stars) or with zero perturbation of the main part of cloudiness (solid line with triangles).

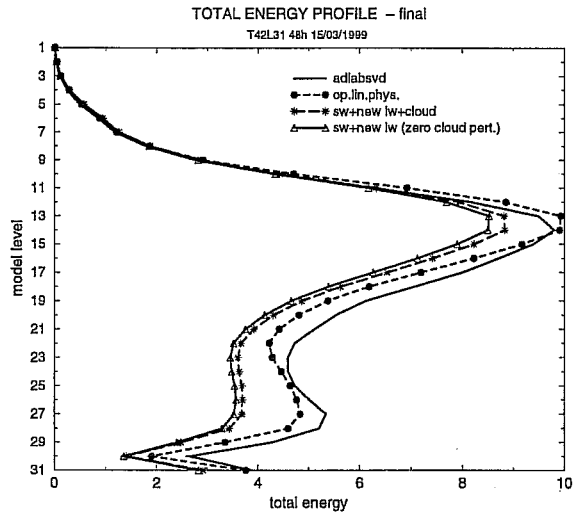

Figure 12: Vertical distribution of total energy spectrum at the final time (after a 48-hour tangent-linear evolution) for the singular vectors computed using the same linearized models as in Fig. 10.